Interfacial thermal resistance between high-density polyethylene (HDPE) and sapphire*

Zheng Kun(郑 鲲)[a)c)], Zhu Jie(祝 捷)[b)†], Ma Yong-Mei(马永梅)[a)‡], Tang Da-Wei(唐大伟)[b)], and Wang Fo-Song(王佛松)[a)]

[a)] *Institute of Chemistry, Chinese Academy of Sciences, Beijing* 100190, *China*
[b)] *Institute of Engineering Thermophysics, Chinese Academy of Sciences, Beijing* 100190, *China*
[c)] *University of Chinese Academy of Sciences, Beijing* 100190, *China*

(Received 12 March 2014; revised manuscript received 14 April 2014; published online 20 August 2014)

To improve the thermal conductivity of polymeric composites, the numerous interfacial thermal resistance (ITR) inside is usually considered as a bottle neck, but the direct measurement of the ITR is hardly reported. In this paper, a sandwich structure which consists of transducer/high density polyethylene (HDPE)/sapphire is prepared to study the interface characteristics. Then, the ITRs between HDPE and sapphire of two samples with different HDPE thickness values are measured by time-domain thermoreflectance (TDTR) method and the results are $\sim 2\times10^{-7}$ m^2·K·W^{-1}. Furthermore, a model is used to evaluate the importance of ITR for the thermal conductivity of composites. The model's analysis indicates that reducing the ITR is an effective way of improving the thermal conductivity of composites. These results will provide valuable guidance for the design and manufacture of polymer-based thermally conductive materials.

Keywords: polymer composites, interfacial thermal resistance, time domain thermalreflectance

PACS: 73.63.Rt, 68.55.Jd, 82.35.Np **DOI:** 10.1088/1674-1056/23/10/107307

1. Introduction

With the continuous increasing in power density of electronic device and the shrinking of device volume to a micro-nano scale, the heat dispersion in microelectronic packaging material has become a thorny problem.[1] Polymeric materials with excellent electronic insulation have been widely used in aforementioned areas due to their good process ability, light weight, and low cost. However, the low thermal conductivity of polymeric packing material restricts the further improvement in its performance, thereby reducing the reliability of the device. Therefore, a large number of studies have been conducted to enhance thermal conductivity of polymeric material by incorporating high thermally conductive fillers into a polymer matrix, but the results are unsatisfactory. The thermal conductivity of prepared composites is enhanced from about 0.2 W·m^{-1}·K^{-1} only to about 2.5 W·m^{-1}·K^{-1}, this is much lower than that of the filler, which ranges from tens to thousands W·m^{-1}·K^{-1}.[2–6] More interestingly, when the thermal conductivity rate of filler to polymeric matrix is larger than 100, the thermal conductivity of the prepared polymeric composites could not be further improved by merely increasing thermal conductivity of the filler.[7] Consequently, the interfacial thermal resistance (ITR) in composites has become a more important property for researchers to concentrate on, and it is considered as a bottle neck to enhancing thermal conductivity of polymeric composites.

Computational studies show that if the interfacial thermal resistance is eliminated, then the thermal conductivity of polymeric composites could be much higher.[8] In some papers the researchers have used an indirect method to estimate the ITR effects in composites. For example, filler treated with couple-agent strengthens the interfacial force, thereby enhancing the thermal conductivity of polymeric composite by approximately 5%, but this is still quite low compared with the thermal conductivity of the filler.[9,10]

However, characterizing heat transport across an interface at a nano-scale is an open challenge, and there are few studies in which the thermal conductivity of polymeric composite at filler-polymer interface has been directly measured, which means that the ITR in polymeric composites remains unknown. The TDTR method is an excellent way to measure ITR,[11,12] by using which the ITR of metal/non-metal was successfully measured.[13,14] Besides, the thermal conductivity of polymer nano-thin-films has also recently been measured by the TDTR method,[15] but the ITR of polymer/inorganic is seldom studied.

In the polymeric composite, there is a large area of interface, which is recognized as a main heat transfer barrier. In this paper, we demonstrate an indirect method to investigate the ITR in polymeric composites, which could be used as guidance for improving the thermal conductivity of a polymeric composite. In detail, we take the alumina filled high density

*Project supported by the National Natural Science Foundation of China (Grant Nos. 51373184 and 51206167), the National Plan for Science & Technology Support, China (Grant No. 2014BAC03B05), and the National Basic Research Program of China (Grant Nos. 2014CB931803 and 2012CB933801).

†Corresponding author. E-mail: mailto:zhujie@iet.cn
‡Corresponding author. E-mail: maym@iccas.ac.cn

© 2014 Chinese Physical Society and IOP Publishing Ltd

polyethylene (HDPE) composite as an example to study the heat transport cross the alumina/HDPE interface. Specifically, a sandwich structure model describing the characteristics of interface in polymeric composite, transducer/HDPE/sapphire, is designed and the relevant samples to be used in this study are prepared. Afterwards, we use TDTR method to acquire the heat attenuation signal in the transducer layer. Then, a heat transfer model is used to fit the signals, and the ITR between HDPE and sapphire is obtained. In addition, the importance of ITR in composite is evaluated by a model.

2. Experiment

2.1. Sample preparation

2.1.1. Materials

Sapphires (0001) were supplied by Hefei Kejing Materials Technology CO., LTD. The dimensions of the sapphires used in this study were 1 cm in length, 1 cm in width, 400 μm in thickness, and the surface roughness was less than 0.4 nm. The high density polyethylene (HDPE) used in this study was 5000S (SinoPec Beijing Yansan Petrochemical Co. Ltd, Beijing, China), with a density of 0.95 g·cm^{-3} and a melt flow index of 0.9 g/10 min (2.16 kg at 190 °C). Decalin was purchased from National Medicine Corporation without further purification prior to use.

2.1.2. Preparation and structure characterization of HDPE films

A series of sandwich structure samples, transducer/HDPE/sapphire, were carefully fabricated. At the first step, HDPE was dissolved in decalin with a concentration of 1 mg·ml^{-1} at 180 °C for at least one hour under nitrogen atmosphere.[16] All the HDPE thin films were prepared on the sapphire substrates via the spin-coating method. The substrates had been carefully cleaned in a standard cleaning procedure: ultrasonic treatment in acetone, isopropanol, and ultra-filtered water (Milli-Q), blown-dry with nitrogen in sequence. All the necessary equipment (sapphire, pipets, spin coater) were preheated to a typical temperature, 180 °C.[16,17] The spin coater with a rotation heater plate could maintain the desired temperature, which allowed us to prepare high-quality HDPE films. The typical rotation speed used in this work was 2000 rpm–3000 rpm. The surface roughness values of HDPE thin films were required to be very small, normally smaller than 10 nm, in order to meet the requirements of TDTR measuring condition.

Atomic Force Microscopy (AFM), Bruker Nanoscope V Multimode 8, with tapping model was used to measure the surface roughness (R_a) of the prepared HDPE thin films. The prepared samples with small surface roughness values met the requirements of TDTR measuring condition.

The thickness of the HDPE thin film must be measured accurately because the thickness of the HDPE film is one of the most significant parameters used for fitting. Here, we employed ellipsometry to measure the thickness values of the thin films, during which measurement the samples were not destroyed. The instrument was preheated for at least one hour prior to measurement.

2.1.3. Preparation of transducer layer

The transducer layer is Al film with a thickness of approximately 100 nm. In order to improve the quality of the transducer layer, 2-nm-thick Ti film was used as an adhesion layer between the Al film and HDPE film to be measured. Firstly, Ti was deposited by thermal evaporation method on polymer film in very high vacuum (∼10^{-4} Pa), and then an Al layer was immediately deposited on Ti layer at a rate of 0.1 Å·s^{-1}. In the deposition process, controlling the temperature below 80 °C would avoid damaging the HDPE film. Two pieces of sapphire substrate were placed next to the sample in the deposition chamber to calibrate the thickness of the Al layer.

2.2. TDTR system

In this paper, the time domain thermoreflectance (TDTR) technique was employed to measure interfacial thermal resistance (ITR).[12,18,19] The experimental setup is schematically shown in Fig. 1. In our measurement we used an 80-MHz Ti:sapphire laser with a full width at half-maximum (FWHM) pulse width of 100 fs. The laser beam was split into pump and probe beams, with their intensity ratio being around 10:1. The pump beam passed through an electro–optic modulator (EOM), which modulated the pulse train at a frequency of 1 MHz, serving as a reference to the signals extracted from the lock-in amplifier. The second-harmonic generator was used to double the frequency of the pump pulses, which produced a light train with a central wavelength of 400 nm. Simultaneously, the probe beam (800 nm) was time-delayed relative to the pump

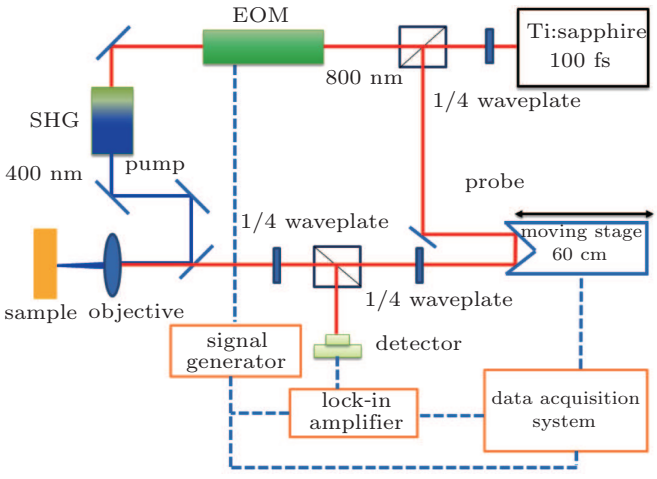


Fig. 1. (color online) Experimental setup of TDTR system.

beam by passing through a mechanical stage. A lock-in amplifier was employed to monitor the reflectance response at the modulated frequency.

2.3. Heat transfer model and lock-in signal

The heat transfer model based on the transform matrix method of heat transfer through multilayers and interfaces has been presented in a previous paper,[12] and here we present some of the key equations simply for the readers to easily understand the rest of the paper.

2.4. Single layer and interface

In each layer, considering a cylindrical heating spot on the surface, the heat conduction equation can be expressed as follows:

$$\frac{k_r}{r}\frac{\partial}{\partial r}\left(r\frac{\partial\widetilde{\theta}}{\partial r}\right)+k_z\frac{\partial^2\widetilde{\theta}}{\partial z^2}=\rho c\frac{\partial\theta(l)}{\partial t}, \tag{1}$$

where r is the radical coordinate, z is the cross-plane coordinate (in the depth direction), t is the time, $\widetilde{\theta}$ is the temperature, ρ is the density, c is the specific heat, and k_r and k_z are the in-plane and cross-plane thermal conductivities, respectively.

Let θ and F be the temperature and heat flux at the face $z=0$ and θ' and F' be their values at the face $z=d$, respectively. The four quantities, θ, F, θ', F', and interfacial thermal resistance R can be related by

$$\begin{bmatrix}\theta'\\ \theta\end{bmatrix}=\begin{bmatrix}1 & -R\\ 0 & 1\end{bmatrix}\begin{bmatrix}\theta\\ F\end{bmatrix}. \tag{2}$$

2.4.1. Multilayer structure

In a multilayer structure with n parallel layers inside, from Eq. (2) we can see that for either a film or an interface at j-th ($j=1,\ldots,n$) layer, the temperature θ_{j+1} on the bottom side of the layer should be the heat flux F_{j+1} on the bottom side of the layer, which should be the product of the temperature θ_j and heat flux F_j on the top side with a matrix M_j, like

$$\begin{bmatrix}\theta_{j+1}\\ F_{j+1}\end{bmatrix}=\begin{bmatrix}A_j & B_j\\ C_j & D_j\end{bmatrix}\begin{bmatrix}\theta_j\\ F_j\end{bmatrix}=M_j\begin{bmatrix}\theta_j\\ F_j\end{bmatrix}. \tag{3}$$

Multiple layers are handled by multiplying the matrix for individual layer together. Therefore, the temperature θ_{n+1} and heat flux F_{n+1} on the bottom side of the multilayer stack can be expressed by

$$\begin{bmatrix}\theta_{n+1}\\ F_{n+1}\end{bmatrix}=\begin{bmatrix}A & B\\ C & D\end{bmatrix}\begin{bmatrix}\theta_1\\ F_1\end{bmatrix}, \tag{4}$$

where θ_1 and F_1 are the temperature and heat flux on the top side of the multiplayer stack, respectively.

The surface temperatures are measured by thermoreflectance; that is, the change in the reflectivity, which depends on temperature. This change in reflectivity is measured by the change in the reflected intensity of a probe laser beam. Let Q_{pump} be the power absorbed from pump laser, and R_{pump} be the $1/e^2$ radius of pump intensity distribution as a Gaussian spot. Let Q_{probe} be the power of probe beam and R_{probe} be the $1/e^2$ radius of probe intensity distribution (Gaussian type). The frequency-domain response $\widetilde{H}(\omega)$ of the surface temperature change in real space can then be expressed as

$$\widetilde{H}(\omega) = -v\frac{Q_{\text{pump}}Q_{\text{probe}}}{2\pi}\int_0^\infty l\left(\frac{D}{C}\right)\times\exp\left[\frac{-l^2\left(R_{\text{pump}}^2+R_{\text{probe}}^2\right)}{8}\right]\mathrm{d}l, \tag{5}$$

where C and D are calculated via Eq. (4).

2.4.2. Lock-in amplifier response

A lock-in amplifier picks up the fundamental harmonic component of probe signal $\widetilde{Z}(\omega_0)$ at the modulation frequency ω_0 and rejects all of the other components. In the case of pulsed pump and probe beams, at each individual delay time τ between pump and probe pulse, $\widetilde{Z}(\omega_0)$ should be given as

$$\widetilde{Z}(\omega_0)=\sum_{m=-\infty}^{\infty}\widetilde{H}(\omega_0+m\omega_{\text{s}})\exp(\mathrm{i}m\omega_{\text{s}}\tau), \tag{6}$$

by using the sampling theorem.[7,20] Here, ω_{s} is the probe pulsing frequency or sampling frequency (80 MHz in our experiment), τ is the delay time between probe and pump pulses, and $\widetilde{H}(\omega)$ is the sample frequency response obtained by Eq. (5).

The output of the lock-in amplifier contains the real part and imaginary part of the fundamental component of the probe signal with respect to the reference wave $\exp(\mathrm{i}\omega_0 t)$, which correspond to the in-phase signal V_{in} and out-of-phase signal V_{out}, respectively:

$$V_{\text{in}}=\mathrm{Re}\left[\widetilde{Z}(\omega_0)\exp(\mathrm{i}\omega_0 t)\right], \tag{7}$$

$$V_{\text{out}}=\mathrm{Im}\left[\widetilde{Z}(\omega_0)\exp(\mathrm{i}\omega_0 t)\right]. \tag{8}$$

The ratio between the in-phase and out-of-phase signal, $-V_{\text{in}}/V_{\text{out}}$, is used to obtain the thermophysical properties by fitting the measurement data to the theoretical model since it is a more robust quantity than amplitude signal.[21]

The model presented above describes the heat transfer process through multilayer structures in the time-domain. In the TDTR measurement, the modulation frequency ω_0 is fixed and the signal is obtained by changing the delay-time τ.

3. Experimental results

In the sandwich structure of transducer/HDPE/sapphire, the ITR between Al and HDPE ($R_{\text{Al/HDPE}}$) as well as the ITR between HDPE and sapphire ($R_{\text{HDPE/sapphire}}$) are the free parameters in our data analysis. The thermal resistance of the 2-nm-thick Ti layer serving as adhesive function between Al and HDPE is involved in $R_{\text{Al/HDPE}}$ during fitting.[21] The thermal

properties of the metal Al film and HDPE film are assumed to be the same as those of bulk Al and bulk HDPE during fitting. The values of surface roughness (R_a) of prepared 120.4-nm and 155.2-nm HDPE films are 8.7 nm and 4.8 nm, respectively, which are shown in Table 1. To ensure the data accurate, we calibrate the system and the data fitting procedure by measuring many samples of well-known materials, that is, silicon and sapphire, prior to measuring the samples. Scans were performed at least three times and the measurements of each sample are averaged to reduce the measurement uncertainty. Figure 2 shows the thermal reflectance responses for samples and the corresponding best fit curves by using the mentioned heat transfer model (Subsection 2.3). The given values and the fitted values are listed in Table 1. The values of ITR between sapphire and HDPE with the thickness (T_{HDPE}) values of 120.1 nm and 155.2 nm are 1.4×10^{-7} $m^2\cdot K^{-1}\cdot W^{-1}$ and 2.0×10^{-7} $m^2\cdot K^{-1}\cdot W^{-1}$, respectively. The difference in ITR might be due to the difference in surface roughness.[13,22]

Table 1. Given and fitted values.

No.	Given values						Fitted values	
	T_{HDPE} /nm	R_a /nm	k_{HDPE} /W·m^{-1}·K^{-1}	C_{HDPE} /J·m^{-3}·K^{-1}	k_{Al} /W·m^{-1}·K^{-1}	C_{p-Al} /J·m^{-3}·K^{-1}	$R_{Al/HDPE}$ /m^2·K·W^{-1}	$R_{HDPE/sapphire}$ /m^2·K·W^{-1}
1	155.2	4.8	0.45	1.7×10^6	230	2.3×10^6	6.3×10^{-8}	2.0×10^{-7}
2	120.4	8.7	0.45	1.7×10^6	230	2.3×10^6	6.3×10^{-8}	1.4×10^{-7}

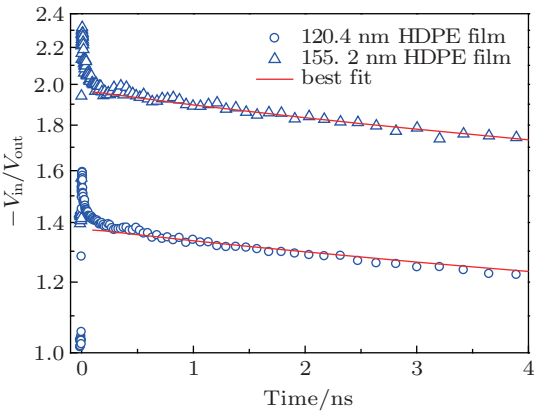


Fig. 2. (color online) TDTR signals $-V_{in}/V_{out}$ of 120-nm- and 150-nm-thick HDPE films and the best fitting to the theoretical thermal conduction model.

4. Model and analysis

In order to evaluate the role of ITR in thermal property of filler incorporated HDPE composite, a simplified model is used for analysis. As shown in Fig. 3, the model is composed of HDPE matrix and an encapsulated cubic filler. Heat flux flows through the model in one direction: from top face to bottom. The total heat flux (f) is grouped into two components, namely, f_1 and f_2, where f_1 represents the heat flux passing through the matrix, HDPE/filler interface, filler, filler/HDPE interface, and HDPE sequentially; and, f_2 denotes the heat flux passing through the remaining parts.

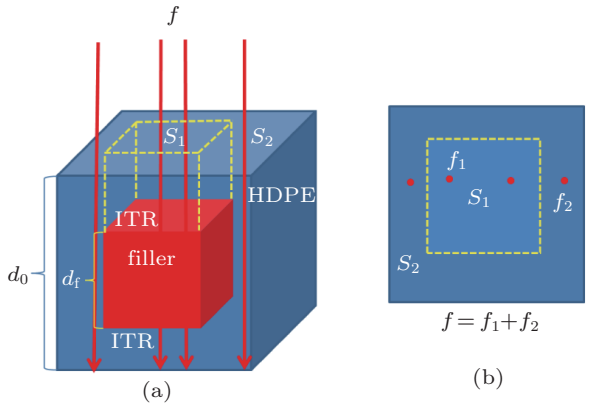


Fig. 3. (color online) Schematic diagram of the heat transfer model, showing (a) the single cubic filler encapsulated in HDPE matrix and (b) the top view of the former.

According to the principle of heat transfer law, the heat flux from the model can be expressed as

$$f_1 = \frac{\lambda_1 \times S_1}{d_0} \times \Delta T, \tag{9}$$

$$f_2 = \frac{\lambda_2 \times S_2}{d_0} \times \Delta T, \tag{10}$$

where λ_2 is the thermal conductivity of HDPE; λ_f is the thermal conductivity of the filler; S_1 and S_2 are the surface areas of filler and the remaining parts; d_0 is the side length of the cubic model; and, d_f is the side length of the cubic filler. λ_1, S_1, S_2, and d_0 can be expressed as follows:

$$\lambda 1 = \frac{d_0}{2\times\dfrac{d_0-d_f}{\lambda_2} + 2R_i + \dfrac{d_f}{\lambda_f}}, \tag{11}$$

$$S_1 = d_f^2, \quad S_2 = d_0^2 - d_f^2, \tag{12}$$

$$d_0 = \sqrt[3]{\frac{d_f^3}{V_f}}. \tag{13}$$

The total heat flux (f) can be expressed as

$$f = f_1 + f_2 = \left(\frac{\lambda_1 \times S_1}{d_0} + \frac{\lambda_2 \times S_2}{d_0}\right) \times \Delta T. \tag{14}$$

The total heat flux can also be express as

$$f = \frac{\overline{\lambda}_0 \times (S_1 + S_2)}{d_0} \times \Delta T, \tag{15}$$

where $\overline{\lambda}_0$ is the effective thermal conductivity of the composite. Combining Eq. (14) and Eq. (15), $\overline{\lambda}_0$ can be given as

$$\overline{\lambda}_0 = \frac{\lambda_1 \times S_1 + \lambda_2 \times S_2}{S_1 + S_2}. \tag{16}$$

The effective interfacial area density S_d in the composite is presented by

$$S_d = \frac{2d_f^2}{d_0^3}. \quad (17)$$

Figure 4 shows the relationships between effective thermal conductivity of composite ($\overline{\lambda}_0$) and the side length of cubic filler (d_f) at different filler volume fractions. In Fig. 4, the cubic filler used is alumina. As can be seen in Fig. 4, $\overline{\lambda}_0$ values clearly vary with d_f at all volume fractions of filler (V_f), they especially vary strongly in the higher V_f case. $\overline{\lambda}_0$ is quadrupled with d_f ranging from 50 nm to 5000 nm when V_f is 50%. This could be reasonably understood because the interface surface area in composite decreases with the increase of d_f, contributing to the enhancement of $\overline{\lambda}_0$ value.

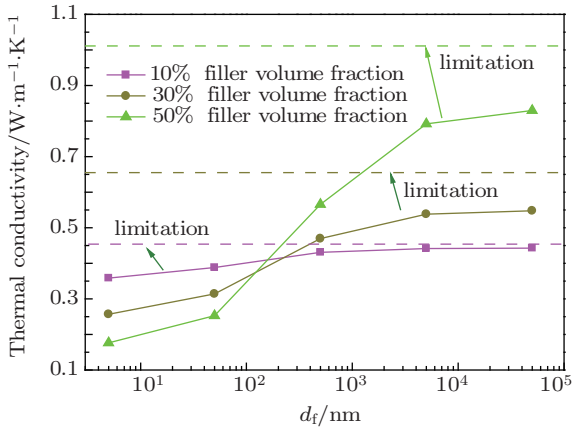


Fig. 4. (color online) Variations of effective thermal conductivity of composites with d_f at different filler volume fractions when ITR is 2.0×10^{-7} $m^2 \cdot K \cdot W^{-1}$ and the thermal conductivity of filler is 30 $W \cdot m^{-1} \cdot K^{-1}$.

It should be noticed that the curves cross each other in a range between 100 nm and 200 nm in Fig. 4. If the side length of filler (d_f) is smaller than 100 nm, then the relatively high rate of interfacial area to the volume of the composite (S_d) makes ITR dominate the thermal conductivity of the composite. In this case, the effective thermal conductivity of the composite with higher filler fraction is smaller than with lower one because the rate of the interfacial area increases with the augment of V_f. In another case, if the d_f is larger than 200 nm, S_d is relatively low, which makes the thermal conductivity of fillers dominate the effective thermal conductivity of the composite. So, the effective thermal conductivity of the composite with higher filler content is larger than with a lower one. Therefore, the curves cross each other in a range between 100 nm and 200 nm, as indicated in Fig. 4.

Another important thing to consider are the limitations of thermal conductivities of composites at all the filler content values. The highest limitation of thermal conductivity of composite is around 1 $W \cdot m^{-1} \cdot K^{-1}$, which is much lower than the thermal conductivity of the filler (about 30 $W \cdot m^{-1} \cdot K^{-1}$). This phenomenon could be explained by the fact that the fillers are completely isolated by HDPE in this model. In this situation, the HDPE is a determinative factor for the thermal conductivity of the composite. Therefore, making the fillers contact each other might be an effective way to improve the thermal conductivity of the composite.

According to the discussion of Fig. 4, ITR plays a significant role in improving the thermal conductivity of composite when d_f is smaller than 100 nm. Additionally, an effective way to improve the thermal conductivity of the composite is to make the fillers contact each other.

Figure 5 shows that the thermal conductivity of composite varies with ITR when the filler volume fraction is 30% for each of all the calculations. The thermal conductivity of composite decreases obviously with the increase of ITR for each of all the filler dimensions. Specifically, when the side length of filler is about 5×10^4 nm, the ITR affects the thermal conductivity of composite slightly, as plotted in Fig. 5. This is attributed to the less effective interfacial area density when the side length of the filler is too long. However, when the d_f is reduced to smaller than 5×10^3 nm, the thermal conductivity of composite shows a clear decline tendency with ITR rising. This indicates that the interfacial area increases to a value that is high enough to affect the thermal conductivity of the composite.

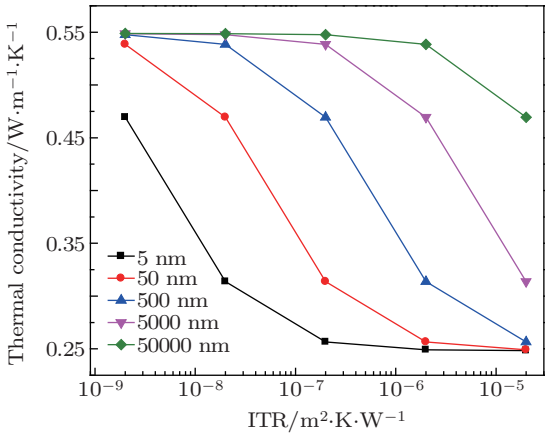


Fig. 5. (color online) Variations of thermal conductivity of composite with ITR side length of filler when filler content is 30%.

The thermal conductivity of composite drops off sharply when the ITR is around 10^{-7} $m^2 \cdot K \cdot W^{-1}$ with the d_f being smaller than 500 nm. In practice, a filler with a wide diameter range is used to prepare a thermal conductive polymeric composite.[2,5,6] Sometimes, big particles with diameters larger than several micrometers are used to prepare relatively high thermal conductive composites at the expense of reducing mechanic performance.[6] Normally, polymers are incorporated with fillers with diameters smaller than tens of micrometers in order to enhance both the thermal conductivity and the mechanical performance at the same time. In other

words, ITR plays a vital role in improving the thermal conductivity by adding fillers with diameters ranging from several nanometers to hundreds nanometers.

All of the discussion about Fig. 5 leads to a view that if the scales of fillers are reduced to nano-scale, the ITR is a determinative key in enhancing the thermal conductivity of composite. A similar phenomenon has been found in carbon nanotubes that are filled with a polymeric matrix.[23]

Figure 6 shows that the thermal conductivities of composites change little with the thermal conductivities of fillers ranging from 20 $W\cdot m^{-1}\cdot K^{-1}$ to 3000 $W\cdot m^{-1}\cdot K^{-1}$ at two different side lengths. This phenomenon accords well with previous experimental results.[7] In other words, it is ineffective to load fillers with high thermal conductivity to a polymer matrix with the hope of improving the thermal conductivity of the prepared materials if the thermal conductivity of the filler is larger than 200 $W\cdot m^{-1}\cdot K^{-1}$, according to the model used.

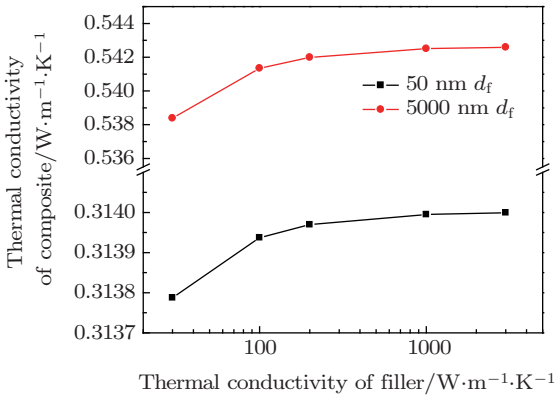


Fig. 6. (color online) Variations of thermal conductivity of composite with thermal conductivity of filler at different side lengths of filler, with filler volume fraction being 30%.

In real polymeric composites the fillers in polymer matrix are distributed randomly. For example, the fillers probably contact each other and are not uniformly distributed. Moreover, the shape of the filler does not have a regular form, as used in this model. All of these factors need to be considered in order to well estimate the thermal conductivity of polymer based composites, but this is beyond this paper. Nevertheless, our simple model shows that ITR and thermal conductivity of the filler both affect the thermal conductivity of a composite.

5. Conclusions

In this paper, we measure the interfacial thermal resistance (ITR) of HDPE/sapphire for the first time by the TDTR method. The ITR of HDPE/sapphire is $\sim 2\times 10^{-7}$ $m^2\cdot K\cdot W^{-1}$. Furthermore, we evaluate the importance of ITR in composite by a model, in which other factors are not considered, such as the filler shape, the diameter distribution, and the gathering of fillers. Our model analysis shows that the thermal conductivity is affected largely by the dimension scale of filler, especially in the case of high filler loading. Strictly speaking, it is ineffective to enhance the thermal conductivity of a polymer simply by loading fillers with a higher thermal conductivity. The model analysis suggests that reducing ITR could be an effective way to enhance the thermal conductivity of a composite. In summary, the thermal conductivity of a composite is quite a complex issue and needs to be further investigated. We believe that this work will provide fundamental guidance for the design and manufacture of thermally conductive polymeric composites.

References

[1] Roy A K, Farmer B L, Varshney V, Sihn S, Lee J and Ganguli S 2012 *ACS Appl. Mater. Interfaces* **4** 545
[2] Weidenfeller B, Höfer M and Schilling F R 2004 *Composites Part A* **35** 423
[3] Wong C P and Bollampally R S 1999 *J. Appl. Polym. Sci.* **74** 3396
[4] Yu S, Hing P and Hu X 2002 *Composites Part A* **33** 289
[5] Zhang S, Cao X Y, Ma Y M, Ke Y C, Zhang J K and Wang F S 2011 *Express Polym. Lett.* **5** 581
[6] Zhou W, Qi S, Tu C and Zhao H 2007 *J. Appl. Polym. Sci.* **104** 2478
[7] Bigg D M 1986 *Polym. Compos.* **7** 125
[8] Cahill D G 2012 *MRS Bull.* **37** 855
[9] Lee G W, Park M, Kim J, Lee J I and Yoon H G 2006 *Composites Part A* **37** 727
[10] Xie S H, Zhu B K, Li J B, Wei X Z and Xu Z K 2004 *Polym. Test.* **23** 797
[11] Cahill D G, Ford W K, Goodson K E, Mahan G D, Majumdar A, Maris H J, Merlin R and Phillpot S R 2003 *J. Appl. Phys.* **93** 793
[12] Zhu J, Tang D, Wang W, Liu J, Holub K W and Yang R 2010 *J. Appl. Phys.* **108** 094315
[13] Hopkins P E, Phinney L M, Serrano J R and Beechem T E 2010 *Phys. Rev. B* **82** 085307
[14] Losego M D, Grady M E, Sottos N R, Cahill D G and Braun P V 2012 *Nat. Mater.* **11** 502
[15] Losego M D, Moh L, Arpin K A, Cahill D G and Braun P V 2010 *Appl. Phys. Lett.* **97** 011908
[16] Wang J, Lu G H, Li L G, Lu Z H, Yang X N and Zhou E L 2008 *Macromolecules* **41** 1273
[17] Wang Y, Ge S, Rafailovich M, Sokolov J, Zou Y, Ade H, Lüning J, Lustiger A and Maron G 2004 *Macromolecules* **37** 3319
[18] Zhu L D, Sun F Y, Zhu J, Tang D W, Li Y H and Guo C H 2012 *Chin. Phys. Lett.* **29** 066301
[19] Zhu L D, Sun F Y, Zhu J and Tang D W 2012 *Acta Phys. Sin.* **61** 134402 (in Chinese)
[20] Capinski W S and Maris H J 1996 *Rev. Sci. Instrum.* **67** 2720
[21] Costescu R M, Wall M A and Cahill D G 2003 *Phys. Rev. B* **67** 054302
[22] Swartz E T and Pohl R O 1989 *Rev. Mod. Phys.* **61** 605
[23] Huxtable S T, Cahill D G, Shenogin S, Xue L, Ozisik R, Barone P, Usrey M, Strano M S, Siddons G, Shim M and Keblinski P 2003 *Nat. Mater.* **2** 731